Am J Physiol Lung Cell Mol Physiol 311: L704–L713, 2016.
First published August 19, 2016; doi:10.1152/ajplung.00005.2016.

Interstitial pneumonia induced by bleomycin treatment is exacerbated in *Angptl2*-deficient mice

Ikuyo Motokawa,[1,6] Motoyoshi Endo,[1] Kazutoyo Terada,[1] Haruki Horiguchi,[1] Keishi Miyata,[1] Tsuyoshi Kadomatsu,[1] Jun Morinaga,[1] Taichi Sugizaki,[1] Takaaki Ito,[2] Kimi Araki,[3] Masaki Suimye Morioka,[4] Ichiro Manabe,[5] Takuya Samukawa,[6] Masaki Watanabe,[6] Hiromasa Inoue,[6] and Yuichi Oike[1]

[1]*Department of Molecular Genetics, Graduate School of Medical Sciences, Kumamoto University, Kumamoto, Japan;* [2]*Department of Pathology and Experimental Medicine, Graduate School of Medical Sciences, Kumamoto University, Kumamoto, Japan;* [3]*Division of Developmental Genetics, Institute of Resource Developmental and Analysis, Kumamoto University, Kumamoto, Japan;* [4]*Department of Bioinformatics, Medical Research Institute, Tokyo Medical and Dental University, Tokyo, Japan;* [5]*Department of Cardiovascular Medicine, Graduate School of Medicine, The University of Tokyo, Tokyo, Japan; and* [6]*Department of Pulmonary Medicine, Graduate School of Medical and Dental Sciences, Kagoshima University, Kagoshima, Japan*

Submitted 5 January 2016; accepted in final form 12 August 2016

Motokawa I, Endo M, Terada K, Horiguchi H, Miyata K, Kadomatsu T, Morinaga J, Sugizaki T, Ito T, Araki K, Morioka MS, Manabe I, Samukawa T, Watanabe M, Inoue H, Oike Y. Interstitial pneumonia induced by bleomycin treatment is exacerbated in *Angptl2*-deficient mice. *Am J Physiol Lung Cell Mol Physiol* 311: L704–L713, 2016. First published August 19, 2016; doi:10.1152/ajplung.00005.2016.—Angiopoietin-like protein 2 (ANGPTL2) is a chronic inflammatory mediator that, when deregulated, is associated with various pathologies. However, little is known about its activity in lung. To assess a possible lung function, we generated a rabbit monoclonal antibody that specifically recognizes mouse ANGPTL2 and then evaluated protein expression in mouse lung tissue. We observed abundant ANGPTL2 expression in both alveolar epithelial type I and type II cells and in resident alveolar macrophages under normal conditions. To assess ANGPTL2 function, we compared lung phenotypes in *Angptl2* knockout (KO) and wild-type mice but observed no overt changes. We then generated a bleomycin-induced interstitial pneumonia model using wild-type and *Angptl2* KO mice. Bleomycin-treated wild-type mice showed specifically upregulated ANGPTL2 expression in areas of severe fibrosing interstitial pneumonia, while *Angptl2* KO mice developed more severe lung fibrosis than did comparably treated wild-type mice. Lung fibrosis seen following bone marrow transplant was comparable in wild-type or *Angptl2* KO mice treated with bleomycin, suggesting that *Angptl2* loss in myeloid cells does not underlie fibrotic phenotypes. We conclude that *Angptl2* deficiency in lung epithelial cells and resident alveolar macrophages causes severe lung fibrosis seen following bleomycin treatment, suggesting that ANGPTL2 derived from these cell types plays a protective role against fibrosis in lung.

angiopoietin-like protein 2; bleomycin-induced interstitial pneumonia; protecting fibrosis

IDIOPATHIC PULMONARY FIBROSIS is defined as progressive interstitial pneumonia with poor prognosis (15). It is believed that recurrent injury to alveolar epithelial cells and accompanying inflammation weaken tissue repair and promote fibrosis by promoting activation and proliferation of fibroblasts (23). Mechanisms underlying this activity, however, remain unclear, and currently there are few effective treatments for this condition (16, 21). Therefore, understanding these mechanisms could suggest novel therapies.

Lung fibrosis reportedly occurs after abnormal repair responses, likely driven by chronic inflammation (6). Some cytokines and chemokines induced by inflammation amplify inflammatory responses and trigger fibroblast proliferation, which is required for fibrosis development (47), suggesting that suppression of chronic inflammation could inhibit lung fibrosis progression.

Angiopoietin-like proteins (ANGPTLs), which exhibit an NH_2-terminal coiled-coil domain used for oligomerization and a COOH-terminal fibrinogen-like domain, are structurally similar to angiopoietins, which are Tie-2 receptor ligands (22). We previously identified ANGPTL2 as a key mediator of chronic inflammation and associated diseases, such as obesity-related metabolic syndrome (41), cardiovascular disease (20, 42), autoimmune disease (35, 36), carcinogenesis (1, 2), and tumor metastasis (12, 29, 34). However, ANGPTL2 expression and function in lung tissue has remained uncharacterized.

Given its inflammatory role in various diseases, we hypothesized that ANGPTL2 expression might exacerbate lung diseases associated with inflammation. To assess this function, we generated mouse interstitial pneumonia models using wild-type and *Angptl2*-deficient mice and assessed tissue injury. We found that *Angptl2* deficiency exacerbated lung fibrosis caused by bleomycin. Furthermore, treatment of the mouse fibroblast cell line 3T3-L1 with recombinant mouse ANGPTL2 protein repressed induction of thrombospondin 1 (*TSP1*), collagen type I (*COL1*) *A1*, and *COL1A2* mRNAs. Overall, our findings suggest that ANGPTL2 derived from lung epithelial cells and resident alveolar macrophages may protect against excess fibrosis in lung.

MATERIALS AND METHODS

Animals. All animal experiments were performed with the approval of the Institutional Animal Care and Use Committee of Kumamoto University in strict accordance with relevant national guidelines. Only male mice were used for experiments. *Angptl2*-deficient [*Angptl2* knockout (KO)] and wild-type littermates on a C57BL/6N background were used in all experiments as described (41).

Address for reprint requests and other correspondence: M. Endo, Dept. of Molecular Genetics, Kumamoto Univ., 1-1-1 Honjo, Kumamoto 860-8556, Japan (e-mail: enmoto@gpo.kumamoto-u.ac.jp).

1040-0605/16 Copyright © 2016 the American Physiological Society

Downloaded from journals.physiology.org/journal/ajplung (065.021.193.086) on March 8, 2022.

Bleomycin mouse model. Male 9-wk-old *Angptl2* KO and wild-type mice were used. The average body weight for animals in all groups was ~20 grams. Mice were anesthetized with 2% isoflurane (Intervet, Tokyo, Japan) and intraperitoneal pentobarbital sodium (Kyoritsu Seiyaku, Ibaragi, Japan). Mice were intratracheally intubated and administered 5 U/kg (mortality rate 40–50%) (26) or 3.5 U/kg (mortality rate 10%) (38) from a stock solution of 1 U/40 μl 0.9% saline. For bleomycin hydrochloride, 1 unit equals 1.042 mg, according to the manufacturer (Nihon Kayaku, Tokyo, Japan).

Bone marrow transplantation. Mouse bone marrow transplantation (BMT) procedures have been described (20). In brief, wild-type or *Angptl2* KO recipient mice received 9 Gy total body irradiation to eradicate bone marrow (BM) cells and then underwent BMT 1 day later. Thirty days later, recipients were treated with bleomycin.

Quantitative real-time PCR. Total lung RNA was extracted with TRIzol reagent (Life technologies, Carlsbad, CA). Deoxyribonuclease-treated RNA was reverse transcribed with a PrimeScript RT Reagent Kit (Takara Bio, Shiga, Japan). PCR was performed using SYBR Premix Ex Taq II (Takara Bio). PCR products were analyzed with a Thermal Cycler Dice Real Time system (Takara Bio), and relative transcript abundance was normalized to that of ribosomal protein S18 (Rps18). Oligonucleotides used for PCR were as follows: mouse surfactant protein (*SP*)-*A*: forward, 5′-CAGCTTGCAGGCTCTGTGTG-3′, reverse, 5′-ACCATGGTTTCCGGGAGTG-3′; mouse *SP-B*: forward, 5′-GCCAAGTGCTTGATGTCTACCTG-3′, reverse, 5′-ATCCCTGGATTCTGTTCTGGCTTA-3′; mouse *SP-C*: forward, 5′-GCTACATCATGAAGATGGCTCCAG-3′, reverse, 5′-ACACAGGGTGCTCACAGCAAG-3′; mouse *SP-D*: forward, 5′-CCTCAAGGCAAACCAGGTCCTA-3′, reverse, 5′-TGCATGCCAGGAGCACCTAC-3′; mouse *Rps18*: forward, 5′-TTCTGGCCAACGGTCTAGACAAC-3′, reverse, 5′-CCAGTGGTCTTGGTGTGCTGA-3′; mouse transforming growth factor (*TGF*)-*β1*: forward, 5′-GTGTGGAGCAACATGTGGAACTCTA-3′, reverse, 5′-TTGGTTCAGCCACTGCCGTA-3′; mouse *TGF-β2*: forward, 5′-GGAGTTCAGACACTCAACACACCAA-3′, reverse, 5′-GCGGAAGCTTCGGGATTTATG-3′; mouse TGF receptor (*TGFR*)-*1*: forward, 5′-TGCAATCAGGACCACTGCAATAA-3′, reverse, 5′-GTGCAATGCAGACGAAGCAGA-3′; mouse *TGFR-2*: forward, 5′-AAATTCCCAGCTTCTGGCTCAAC-3′, reverse, 5′-TGTGCTGTGAGACGGGCTTC-3′; mouse *COL1A1*: forward, 5′-GACATGTTCAGCTTTGTGGACCTC-3′, reverse, 5′-GGGACCCTTAGGCCATTGTGTA-3′; mouse *COL1A2*: forward, 5′-AGGCTGACACGAACTGAGGT-3′, reverse, 5′-ATGCACATCAATGTGGAGGA-3′; mouse tumor necrosis factor (*TNF*)-*α*: forward, 5′-AAGCCTGTAGCCCACGTCGTA-3′, reverse, 5′-GGCACCACTAGTTGGTTGTCTTTG-3′; mouse interleukin (*IL*)-*6*: forward, 5′-CCACTTCACAAGTCGGAGGCTTA-3′, reverse, 5′-GCAAGTGCATCATCGTTGTTCATAC-3′; mouse *CD68*: forward, 5′-CATCAGAGCCCGAGTACAGTCTACC-3′, reverse, 5′-AATTCTGCGCCATGAATGTCC-3′; and mouse *TSP1*: forward, 5′- CGAGTTGCAAAGGGAGATGT-3′, reverse, 5′-AGCAGCCTTTGTTCCTGAGA-3′.

Generation of ANGPTL2 monoclonal antibody. Recombinant mouse ANGPTL2 COOH-terminally tagged with hexahistidine (constructed in the pQE vector; Qiagen, Hilden, Germany) was expressed in *Escherichia coli* RosettapLacI cells (Merck, Kenilworth, NJ). Induced protein found in inclusion bodies was washed thoroughly and solubilized in a solution containing 6 M guanidine hydrochloride. Solubilized protein was reduced with 10 mM dithiothreitol and modified by 3-trimethylammoniopropyl methanethiosulfonate bromide (TAPS; Wako, Osaka, Japan) according to a published procedure (43). TAPS-modified proteins were desalted and recombinant protein purified by metal chelating chromatography with a Talon affinity column (Takara Bio). A portion of the purified protein was refolded by dilution in a solution of a mixed disulfide (2 mM cysteine and 0.5 mM cystine) and 2 M sodium lactate, pH 8.0, at 4°C for 14 h under a nitrogen atmosphere. The refolded sample was desalted by reverse-phase chromatography with a Source 30 matrix (GE Healthcare, Little Chalfont, UK). The sample eluted in acetonitrile-0.04% trifluoroacetic acid buffer was freeze-dried and dissolved in 0.1% acetic acid. A sample with an endotoxin level <0.3 EU/mg was stored at −80°C until immunization.

The ANGPTL2 antibody raised in rabbits was generated by a custom service (Abcam, Cambridge, MA). A single hybridoma clone (2E3) was selected for use in immunostaining.

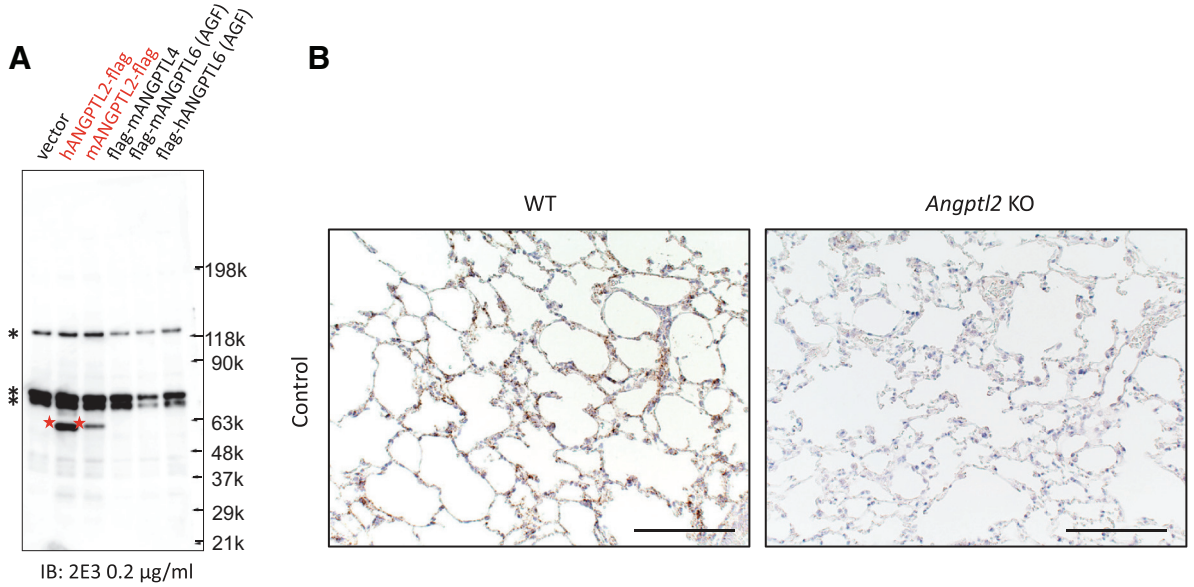

Fig. 1. *A*: immunoblot analysis of human angiopoietin-like protein 2 (ANGPTL2) (hA2-flag), mouse ANGPTL2 (mA2-flag), mouse ANGPTL4 (flag-mA4), mouse ANGPTL6 (flag-mAGF), and human ANGPTL6 (flag-hAGF) protein using an anti-mouse ANGPTL2 monoclonal antibody (RabMAb) (2E3). Red stars and asterisks indicate ANGPTL2 protein and nonspecific bands, respectively. *B*: image showing representative ANGPTL2 2E3 immunostaining in wild-type (WT, $n = 1$ mouse analyzed) or *Angptl2* knockout (KO, $n = 1$ mouse analyzed) mouse lung. Scale bars, 100 μm. Experiments in *A* and *B* were performed one time.

Downloaded from journals.physiology.org/journal/ajplung (065.021.193.086) on March 8, 2022.

Immunohistochemical staining. Dissected mouse lung tissues were fixed in 4% paraformaldehyde/PBS (pH 7.4), washed in PBS for 15 min, dehydrated through a graded series of ethanol and xylene, and embedded in a single paraffin block. Sections (5 μm) were cut, air-dried, deparaffinized, and pretreated with 5 mM periodic acid (Sigma-Aldrich, St. Louis, MO) for 10 min at room temperature to inhibit endogenous peroxidases. Mouse specimens were incubated for 15 h with antibody against mouse ANGPTL2 (2E3, 25 ng/ml) and then washed three times in PBS for 5 min each. Staining was performed using the Tyramide Signal Amplification kit (PerkinElmer, Boston, MA). Light field images were obtained using a BX50 microscope equipped with a DP70 digital camera (Olympus, Tokyo, Japan). For double immunofluorescence, after immunostaining for 2E3, specimens were incubated 15 h with 100-fold diluted antibody against aquaporin 5 (ab78465; Abcam), pro-SP-C (ab40897; Abcam), vimentin (EPR3776; Abcam), or Iba1 (019–19741; Wako). After PBS washing, sections were incubated with Alexa Fluor 488-labeled anti-rabbit IgG (A21206; Life Technologies) and Texas Red-labeled anti-streptavidin (PerkinElmer) as second antibodies. After PBS washing, fluorescent images were obtained using the BZ-H1M system (Keyence, Osaka, Japan).

BAL preparation, ANGPTL2 measurement in BALF, and alveolar cell staining. Bronchoalveolar lavage (BAL) procedures were previously described (11). Mouse lungs were lavaged intratracheally with saline to obtain bronchoalveolar lavage fluid (BALF). Samples were centrifuged at 820 *g* for 5 min at 4°C, and supernatants were assessed by ELISA using an ANGPTL2 Assay Kit (IBL, Gunma, Japan), according to the manufacturer's instructions. To identify alveolar cells, BALF were applied to cytospin slides, which were then centrifuged at 820 *g* for 5 min at room temperature. Alveolar cell staining was performed using Diff-Quik (Sysmex, Hyogo, Japan) according to the manufacturer's protocol, and samples were observed at ×200 magnification using a BX50 microscope equipped with a DP70 digital camera (Olympus). The proportion (percentage) of each type of alveolar cell was calculated based on cell morphology. Ten fields were observed per sample by two observers.

Hydroxyproline assay. Hydroxyproline content of mouse lung was evaluated colorimetrically as described (13), with modifications. Lungs were dissected from other pulmonary structures and homogenized in PBS (0.1 mg tissue/ml). An equal volume of HCl was added, and samples were hydrolyzed at 110°C for 24 h. Five microliters of each sample were mixed with 5 μl of citrate-acetate buffer [5% citric acid (Sigma Aldrich), 1.2% acetic acid, 7.25% sodium acetate, and 3.4% sodium hydroxide]. One hundred microliters of chloramine-T solution [1.4% chloramine-T (Tokyo Chemical Industry, Tokyo, Japan) in 10% 2-propanol and 80% citrate-acetate buffer] were added, and the mixture was incubated for 20 min at room temperature. Ehrlich's solution (Sigma-Aldrich) was added, samples were incubated at 65°C for 18 min, and absorbance at 550 nm was measured. Standard curves were generated for each experiment using hydroxyproline (Wako) as a standard. Results were expressed as milligrams hydroxyproline per gram lung tissue.

Cell culture. The mouse fibroblast cell line 3T3-L1 (IFO50416), purchased from the JCRB Cell Bank (Osaka, Japan), was cultured in Dulbecco's modified Eagle's medium (DMEM; Wako) supplemented with 10% FCS at 37°C in a humidified 5% CO_2 atmosphere. Cells

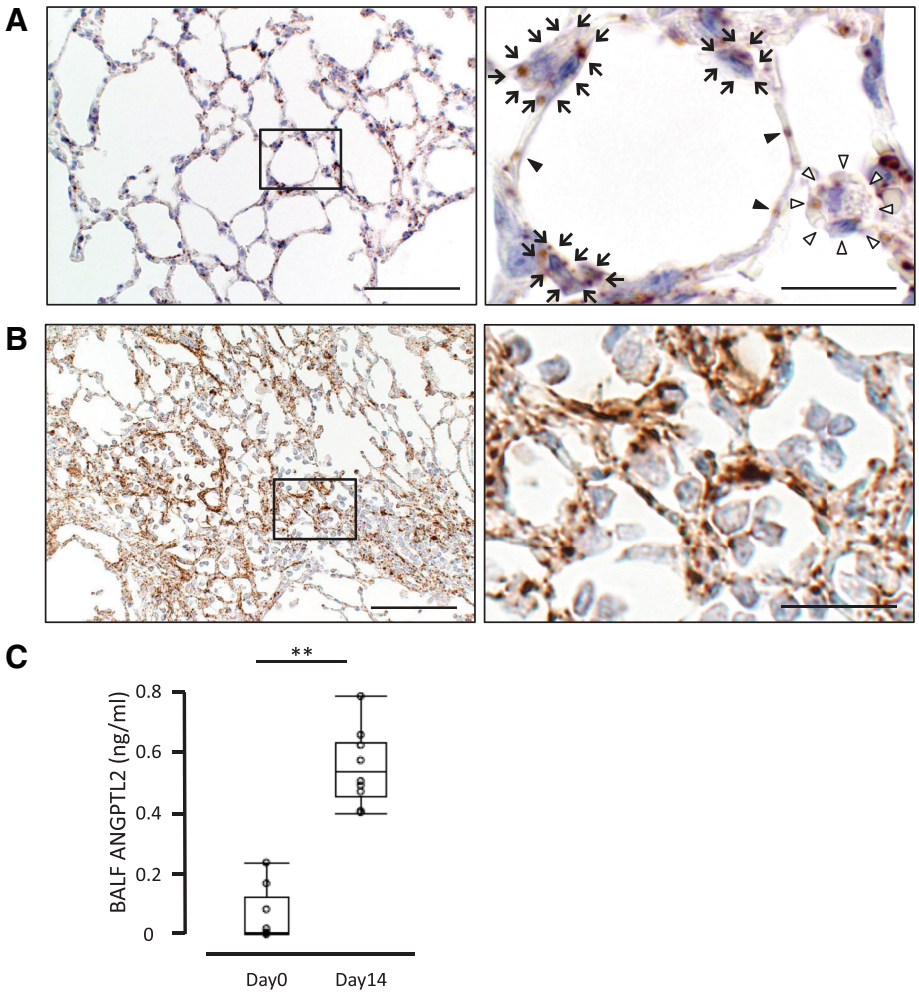

Fig. 2. ANGPTL2 is induced in alveolar epithelial type I and type II cells in a bleomycin-induced mouse interstitial pneumonia model. *A*: image showing representative ANGPTL2 immunostaining in wild-type mouse lung not treated with bleomycin (*left*) ($n = 3$ mice analyzed). *Right*, higher-magnification image of the squared area on *left*. Filled arrowheads indicate alveolar epithelial type I cells, arrows indicate alveolar epithelial type II cells, and open arrowheads indicate an alveolar macrophage. Scale bars, 100 (*left*) and 25 (*right*) μm. *B*: image showing representative ANGPTL2 immunostaining of tissue from wild-type mice within a fibrosing region 14 days after bleomycin treatment (*left*) ($n = 3$ mice analyzed). *Right*, higher-magnification image of squared area on *left*. Scale bars, 100 (*left*) and 25 (*right*) μm. Experiments in *A* and *B* were performed one time. *C*: ANGPTL2 concentrations in bronchial alveolar lavage fluid (BALF) at *days 0* ($n = 10$ mice analyzed) and *14* ($n = 10$ mice analyzed) after bleomycin treatment. Data are means ± SE from one experiment. $^{**}P < 0.01$ (unpaired 2-tailed Student's *t*-test).

Downloaded from journals.physiology.org/journal/ajplung (065.021.193.086) on March 8, 2022.

were plated at 2×10^5 cells/well in DMEM containing 10% FCS, and then medium was changed to fresh medium containing 10 μg/ml rANGPTL2 protein (48) or 0.1% acetic acid (solvent control). Cells were then cultured 24 h before quantitative real-time PCR analysis of genes relevant to collagen synthesis.

RNA sequencing. Sample libraries constructed from lung of wild-type or *Angptl2* KO mice were prepared using a NEBNext Ultra RNA Library Prep Kit for Illumina (New England BioLabs). Sequencing runs were performed on an Illumina Genome Analyzer IIx (Illumina); 38-bp reads were mapped to the human genome (hg19 from the University of California Santa Cruz genome browser database) using TopHat version 2.0.0 (44). Only reads with a Phred quality score ≥25 were analyzed. The BEDtools package (37) was used to filter rRNA and tRNA, with rRNA and tRNA annotations downloaded from the University of California Santa Cruz table browser.

To evaluate differential expression, gene expression data were normalized, and gene annotations were added using the RegionMiner with Genomatix Genome Analyzer (Genomatix, Munich, Germany) software. The normalized expression (NE) value was based on the following formula:

$$NE = 10^7 \times \text{number of reads}_{\text{region}} / \left(\text{number of reads}_{\text{mapped}} \times \text{length}_{\text{region}}\right)$$

(3).

To prepare a list of up- or downregulated genes, all alternative gene transcripts were used to calculate a mean $\log_2$ fold change in gene expression level between wild-type and *Angptl2* KO lungs. This experiment was performed one time. RNA-seq data were deposited in the DDBJ Sequence Read Archive (DRA), with accession number DRA004194.

Statistical analysis. Data are reported as the means ± SE. All simple comparisons were performed using Student's *t*-test, with $P < 0.05$ considered statistically significant.

To compute statistical significance of RNA-seq data, we used the Audic-Claverie algorithm, where a *P* value for enrichment of reads in KO compared with control samples was calculated for each transcript. For multiple testing correction, *P* values were adjusted using the Benjamini and Hochberg method (4).

RESULTS

Generation of a rabbit monoclonal antibody recognizing mouse ANGPTL2. To evaluate ANGPTL2 function in mouse lung, we first generated a new rabbit monoclonal antibody (2E3) that specifically recognizes mouse ANGPTL2 (see MATERIALS AND METHODS). Western blotting confirmed that 2E3 specifically reacts with mouse and human ANGPTL2 protein but not with mouse ANGPTL4 or mouse or human ANGPTL6 (AGF) proteins (Fig. 1*A*). We also confirmed that 2E3 detects ANGPTL2 protein in lung of wild-type but not *Angptl2* KO mice (Fig. 1*B*).

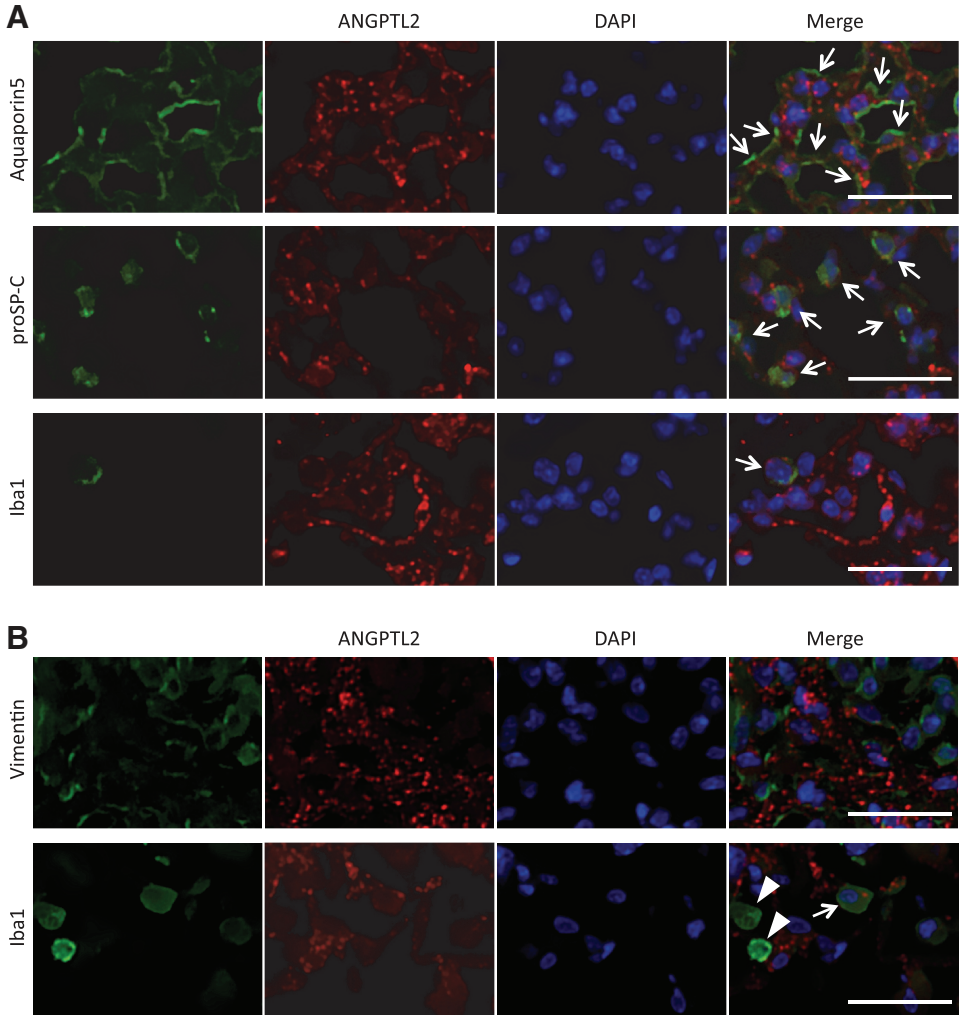

Fig. 3. Fluorescent images of ANGPTL2 and other markers in normal and bleomycin-treated wild-type mouse lung. *A*: representative image of immunohistochemical staining for aquaporin 5 (*top*), pro-surfactant protein C (*middle*), and iba1 (*bottom*) in normal lung tissue ($n = 3$ mice analyzed). *B*: representative image of staining for vimentin (*top*) and iba1 (*bottom*) in bleomycin-treated lung tissue ($n = 3$ mice analyzed). Arrows show cells that express both ANGPTL2 and the marker of interest. Arrowheads show cells that express the marker but not ANGPTL2. Scale bars, 50 μm. Experiments in *A* and *B* were performed one time.

Downloaded from journals.physiology.org/journal/ajplung (065.021.193.086) on March 8, 2022.

ANGPTL2 is upregulated in alveolar epithelial cells in a bleomycin-induced interstitial pneumonia model. To determine which lung cells express ANGPTL2, we immunostained normal mouse lung tissue using the 2E3 antibody (Fig. 2*A*) and observed significant ANGPTL2 expression in both alveolar epithelial type I and type II cells and in resident alveolar macrophages. We then asked whether ANGPTL2 levels increase in bleomycin-induced interstitial pneumonia in wild-type mice after a single administration of bleomycin. We observed that various cells, including alveolar epithelial cells, showed stronger ANGPTL2 positivity in areas exhibiting severe interstitial pneumonia than their counterparts in regions with less tissue damage (Fig. 2*B*). We also observed that ANGPTL2 protein levels in BALF of this model were significantly elevated compared with ANGPTL2 levels in BALF from controls not treated with bleomycin (Fig. 2*C*).

To further examine ANGPTL2 expression in lung cell types, we performed double immunofluorescence in normal lung to assess potential colocalization of ANGPTL2 with aquaporin 5 (a marker of alveolar epithelial type I cells), pro-SP-C (a marker of alveolar epithelial type II cells), and iba1 (a macrophage marker) (Fig. 3*A*). We confirmed that ANGPTL2 is expressed in all three cell types (Fig. 2). We next assessed ANGPTL2-expressing cells in bleomycin-induced interstitial pneumonia (Fig. 3*B*) using vimentin as a marker of mesenchymal cells, including fibroblasts (17), and found that vimentin-expressing cells did not express ANGPTL2. When we checked ANGPTL2 expression in macrophages in the bleomycin model, we found that some macrophages expressed ANGPTL2, but many did not. Because resident alveolar macrophages in normal lung tissue express ANGPTL2, this finding suggests that ANGPTL2 may be expressed by macrophages but not by recently recruited inflammatory monocytes.

Wild-type and Angptl2 KO mice exhibit comparable lung phenotypes. To further assess ANGPTL2 function, we investigated potential lung phenotypes in *Angptl2* KO mice (41). As

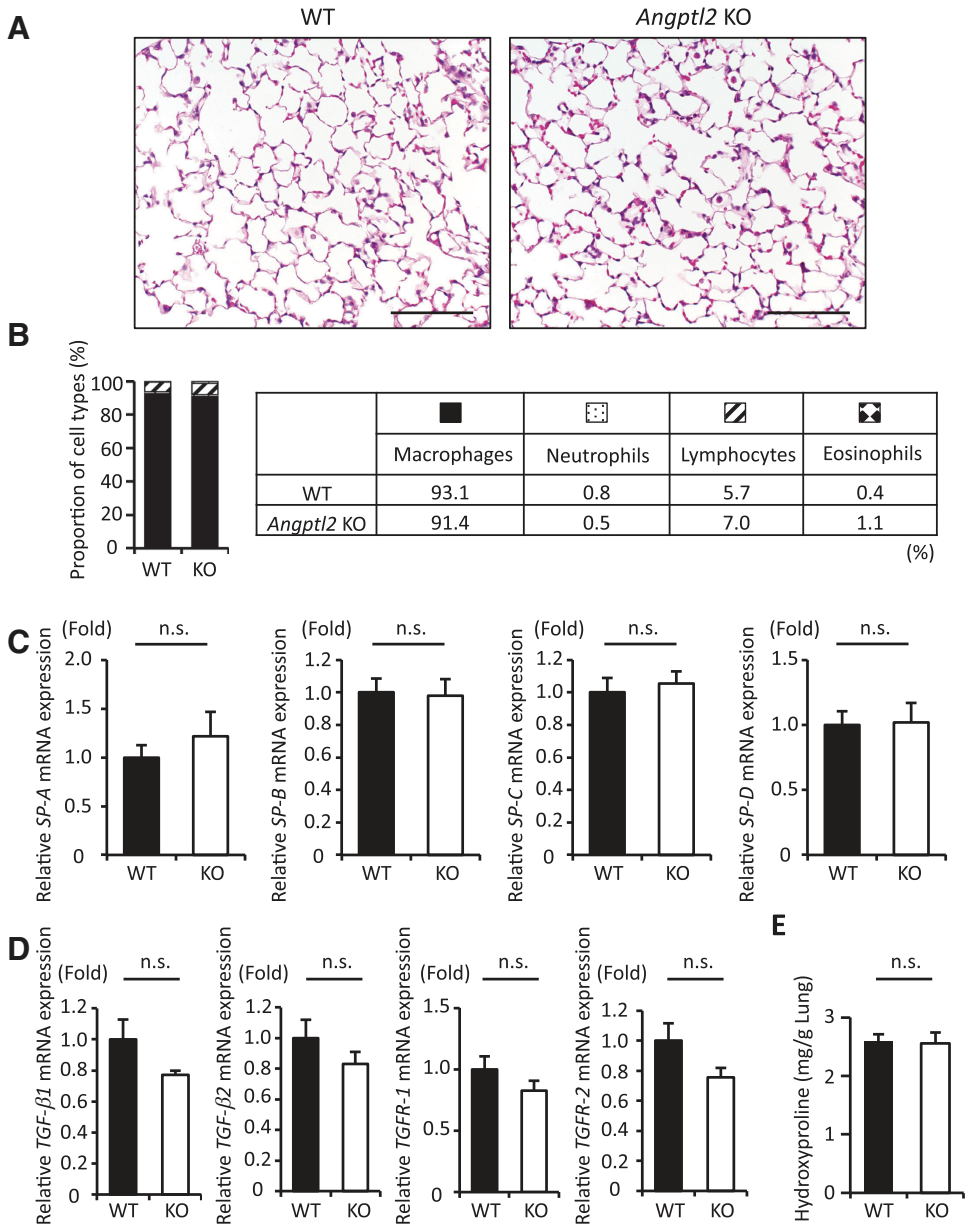

Fig. 4. Lung phenotypes in wild-type and *Angptl2* KO mice. *A*: representative microscopy images of hematoxylin and eosin (H&E)-stained lungs from wild-type ($n = 5$ animals analyzed) and *Angptl2* KO ($n = 5$ animals analyzed) mice not treated with bleomycin. Scale bars, 100 μm. *B*: analysis indicating proportion of macrophages, neutrophils, lymphocytes, and eosinophils in bronchial alveolar lavage fluid of wild-type ($n = 5$ animals analyzed) or *Angptl2* KO ($n = 5$ animals analyzed) mice. Experiments in *A* and *B* were performed one time. *C*: comparative expression of genes encoding various surfactant proteins (SPs) in wild-type ($n = 6$ animals analyzed) and *Angptl2* KO ($n = 6$ animals analyzed) mouse lung. mRNA levels in wild-type mice were set at 1. *D*: comparative expression of genes encoding transforming growth factor (TGF) signaling-related genes in wild-type ($n = 6$ animals analyzed) and *Angptl2* KO ($n = 6$ animals analyzed) mouse lung. mRNA levels in wild-type mice were set at 1. *E*: hydroxyproline content in lung of wild-type ($n = 5$ animals analyzed) and *Angptl2* KO ($n = 5$ animals analyzed) mice not treated with bleomycin. Data are means ± SE from 1 (*E*) or 2 (*C* and *D*) different experiments. ns, Not statistically significant.

Downloaded from journals.physiology.org/journal/ajplung (065.021.193.086) on March 8, 2022.

reported, *Angptl2* KO mice are born alive at Mendelian ratios and appear grossly normal (41). Lungs of *Angptl2* KO mice also showed no apparent morphological changes relative to wild-type mice (Fig. 4*A*), and proportions of alveolar cell subtypes in BALF from wild-type and *Angptl2* KO mice were comparable (Fig. 4*B*). RT-PCR analysis also indicated similar levels of mRNAs encoding SPs (*SP-A*, *SP-B*, *SP-C*, and *SP-D*) in mouse lung of both genotypes (Fig. 4*C*). Expression of TGF family mRNAs (*TGF-β1*, *TGF-β2*, *TGFR-1*, and *TGFR-2*) in lung of wild-type and *Angptl2* KO mice was also comparable (Fig. 4*D*), as was lung hydroxyproline content (Fig. 4*E*). These results suggest that loss of *Angptl2* alone is not sufficient to cause fibrotic phenotypes in lung.

Lung fibrosis induced by bleomycin is potentiated in Angptl2 KO mice. We next asked whether development of lung fibrosis induced by bleomycin is altered in *Angptl2* KO mice. As expected, we observed lung fibrosis in both wild-type and *Angptl2* KO mice 14 days after bleomycin treatment. However, lung fibrosis was greater in *Angptl2* KO relative to wild-type mice at that time point (Fig. 5*A*). In addition, collagen deposition in lung interstitium was greater in *Angptl2* KO compared with wild-type mice (Fig. 5*A*). Moreover, induction of collagen type I (*COL1A1* and *COL1A2*) mRNAs was greater in lungs of *Angptl2* KO mice, as was hydroxyproline content (Fig. 5, *B* and *C*). On the other hand, induction of inflammatory cytokines, such as *TNF-α* and *IL-6*, and of the macrophage marker *CD68* mRNA was comparable in lung of wild-type and *Angptl2* KO mice. We conclude that enhanced lung fibrosis following bleomycin treatment seen in *Angptl2*-deficient mice is likely not due to increased expression of inflammatory factors.

Angptl2 deficiency in alveolar epithelial cells but not myeloid-derived cells accelerates lung fibrosis. Myeloid-derived cells, such as macrophages and neutrophils, play important roles in lung fibrosis (5, 46, 47, 49). To examine whether

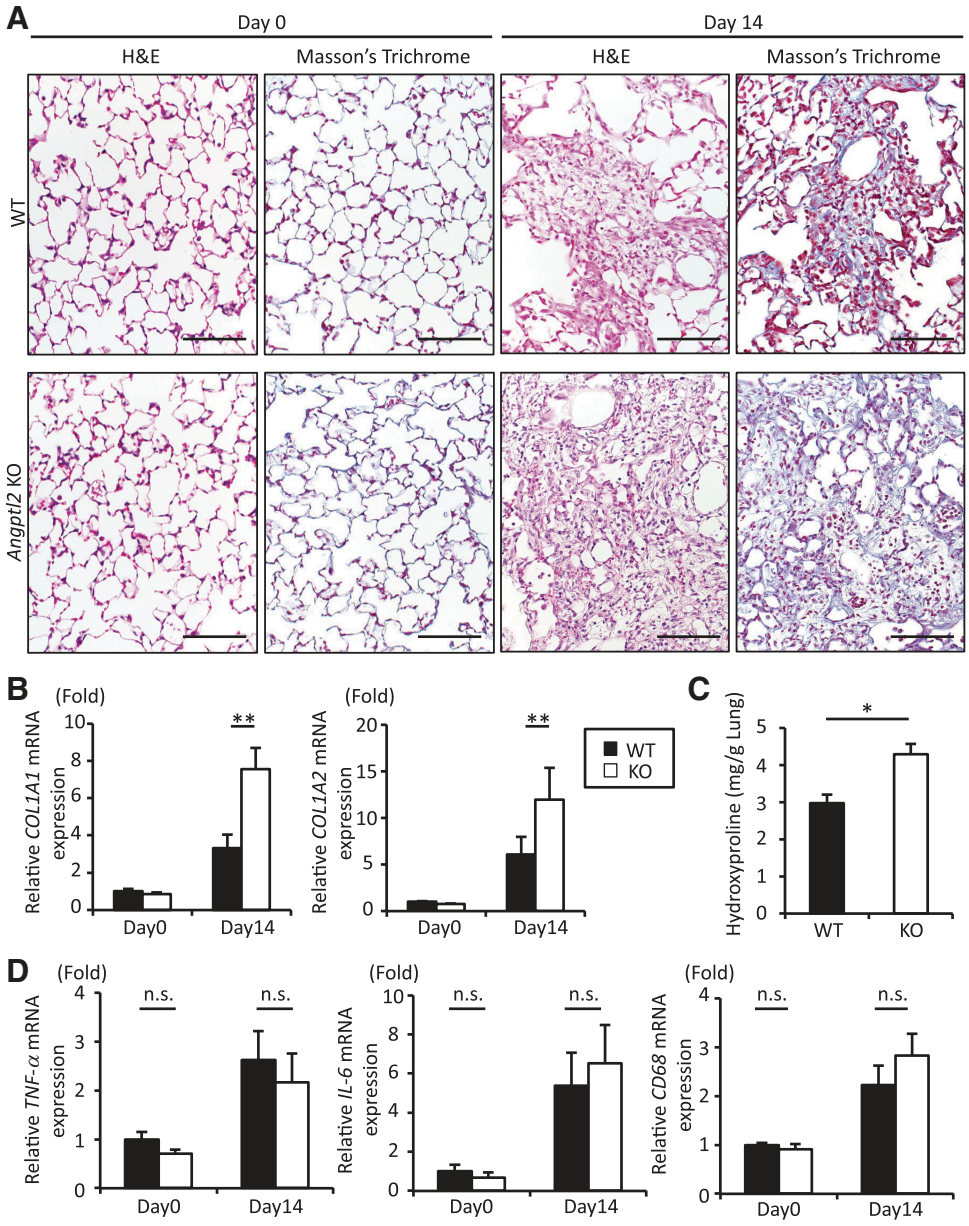

Fig. 5. Lung fibrosis induced by bleomycin treatment is potentiated in *Angptl2* KO mice. *A*: representative microscopy images of H&E- or Masson trichrome-stained lungs of wild-type ($n = 3$ animals analyzed) and *Angptl2* KO ($n = 3$ animals analyzed) mice at *days 0* or *14* after bleomycin treatment. Scale bars, 100 μm. The experiment was performed one time. *B*: comparative expression of genes encoding collagen 1A1 and 1A2 in wild-type ($n = 6$ animals analyzed) and *Angptl2* KO ($n = 6$ animals analyzed) mouse lung. mRNA levels in wild-type mice at *day 0* were set at 1. *C*: hydroxyproline content in lung of wild-type ($n = 4$ animals analyzed) and *Angptl2* KO ($n = 4$ animals analyzed) mice at *day 14* after bleomycin treatment. *D*: comparative expression of genes encoding tumor necrosis factor (TNF)-α, interleukin (IL)-6, and CD68 in wild-type ($n = 6$ animals analyzed) and *Angptl2* KO ($n = 6$ animals analyzed) mouse lung. mRNA levels in wild-type mice at *day 0* were set at 1. Error bars show SE from one (*B*, *C*, and *D*) experiment. $*P < 0.05$ and $**P < 0.01$.

Downloaded from journals.physiology.org/journal/ajplung (065.021.193.086) on March 8, 2022.

Angptl2 deficiency in myeloid-derived cells accelerates lung fibrosis in our model, we performed BMT from either wild-type or *Angptl2* mutant donors into wild-type and *Angptl2* KO recipients and compared bleomycin-induced fibrosis. Figure 6*A* shows both the protocol of the BMT experiment (*top*) and relationships between donors and recipients (*bottom*). Lung fibrosis following bleomycin treatment was significant in *Angptl2* KO recipients transplanted with either wild-type or *Angptl2* KO BM cells (Fig. 6*C*) relative that seen in wild-type recipients (Fig. 6*B*) transplanted with BM from either genotype. On the other hand, the extent of lung fibrosis between recipients of the same genotype did not differ significantly following BMT with cells of either genotype (Fig. 6, *B* and *C*), and hydroxyproline content between recipients of the same genotype also did not differ following transplantation of BMT from either wild-type or *Angptl2* KO mice (Fig. 6*D*). Given that alveolar epithelial cells express ANGPTL2 (Fig. 2*A*), it is likely that ANGPTL2 production by epithelial cells, rather than myeloid-derived cells, may protect lung tissue from fibrosis.

Treatment of mouse fibroblasts with recombinant ANGPTL2 protein decreases TSP1 expression without altering TGF signaling. Given that ANGPTL2 is a secreted protein (12), we asked whether treatment with recombinant mouse ANGPTL2 protein (rANGPTL2) would downregulate TGF-related genes in the mouse fibroblast cell line 3T3-L1 (Fig. 7*A*). However, cells treated with rANGPTL2 did not show changes in expression of TGF family mRNAs (*TGF-β1*, *TGF-β2*, *TGFR-1*, and *TGFR-2*) relative to controls. We then compared gene expression in *Angptl2* KO and wild-type lung by RNA sequencing and identified transcripts whose expression was markedly

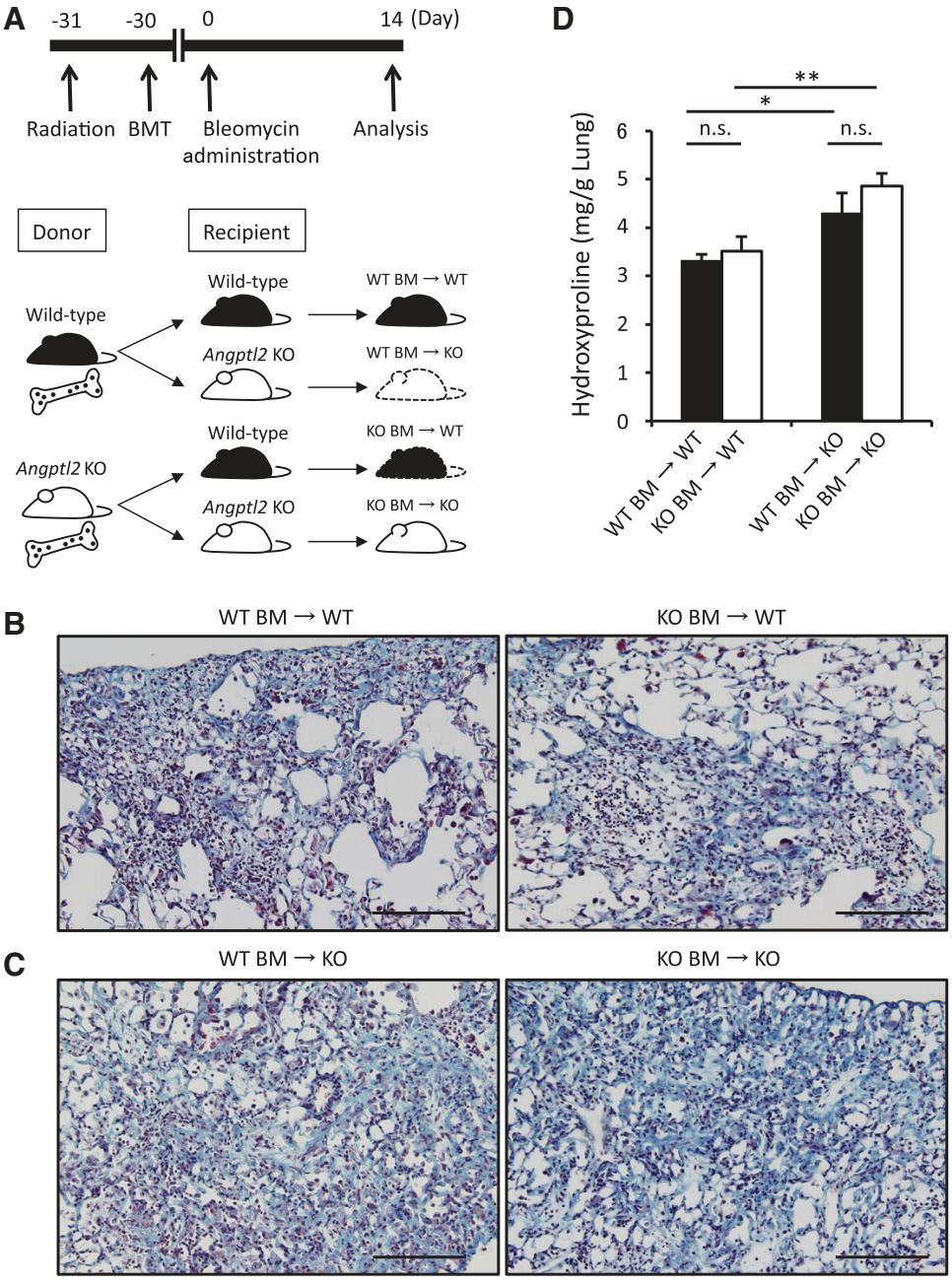

Fig. 6. ANGPTL2 expression in myeloid-derived cells has little effect on fibrosis induced by bleomycin. *A*: diagram showing time course of the BMT experiment (*top*) and relationships between donors and recipients (*bottom*). *B*: representative microscopy images of Masson trichrome-stained lungs at *day 14* after bleomycin treatment in tissues from irradiated wild-type recipients transplanted with wild-type ($n = 3$ mice analyzed) or *Angptl2* KO ($n = 4$ mice analyzed) bone marrow (BM) cells. Scale bars, 100 μm. *C*: representative microscopy images of Masson trichrome-stained lungs 14 days after bleomycin treatment in tissues from irradiated *Angptl2* KO recipients transplanted with wild-type ($n = 3$ mice analyzed) or *Angptl2* KO ($n = 4$ mice analyzed) BM. Scale bars, 100 μm. *D*: hydroxyproline content in lung of wild-type ($n = 3$ animals analyzed) or *Angptl2* KO ($n = 4$ animals analyzed) mice that had undergone BMT. Data are means ± SE from one (*B*, *C*, and *D*) experiment. $*P < 0.05$ and $**P < 0.01$.

Downloaded from journals.physiology.org/journal/ajplung (065.021.193.086) on March 8, 2022.

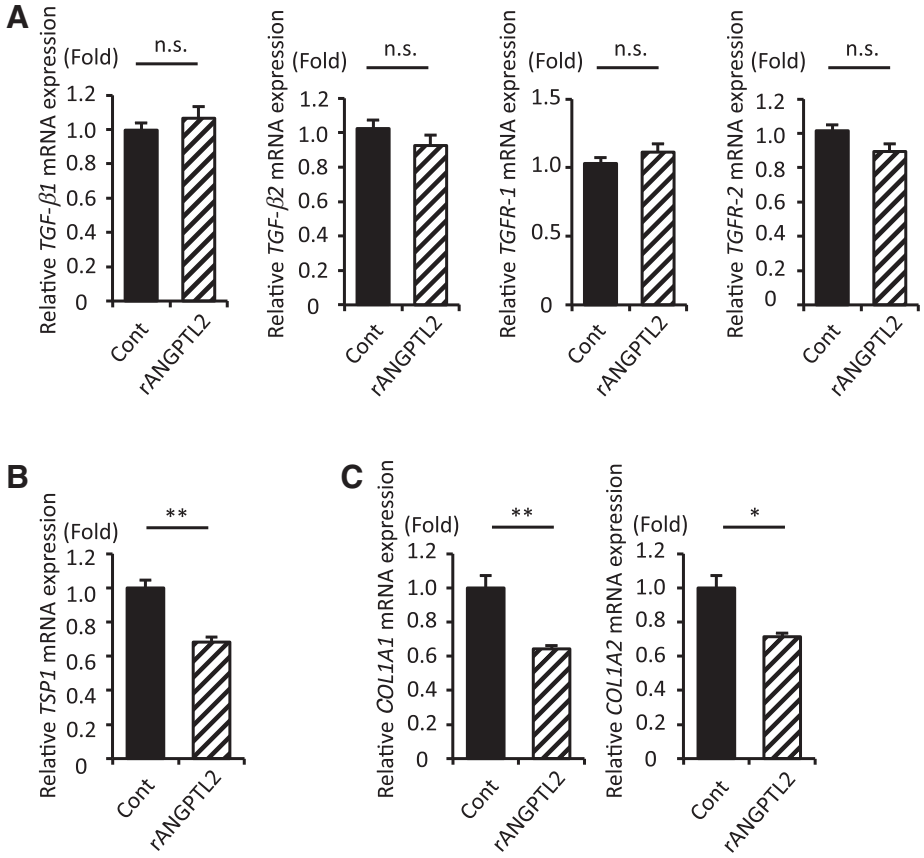

Fig. 7. Effect of recombinant mouse ANGPTL2 protein (rANGPTL2) treatment on fibroblasts. *A–C*: comparative expression of transcripts encoding TGF signaling-related factors (A), thrombospondin 1 (*TSP1*, *B*), and collagen type I (*COL1A1* and *COL1A2* (C) in mouse fibroblast 3T3-L1 cells treated with solvent (Cont) ($n = 6$ plates analyzed) or rANGPTL2 ($n = 6$ plates). mRNA levels in Cont were set at 1. Error bars show SE from two (*A*, *B*, and *C*) different experiments. $^*P < 0.05$ and $^{**}P < 0.01$.

changed by *Angptl2* loss [Supplemental Tables S1 and S2 (Supplemental data for this article may be found on the Journal website.)]. Among them, *Thbs1*, which encodes the TGF-β1-activating factor THBS1 (or TSP1) (32), was upregulated in lung of *Angptl2* KO mice. Moreover, rANGPTL2 treatment of 3T3-L1 cells decreased levels of *TSP1* mRNAs relative to untreated controls (Fig. 7*B*). Accordingly, expression of *COL1A1* and *COL1A2* mRNAs, which are downstream of TGF-β1 signaling, decreased in rANGPTL2-treated 3T3-L1 cells (Fig. 7*C*). These results suggest that ANGPTL2 protein potentially secreted from alveolar cells or macrophages may protect tissues from fibrosis, at least in part, by reducing *TSP1* mRNA in fibroblasts.

DISCUSSION

Here, we show that ANGPTL2 is expressed in alveolar type I cells, type II cells, and alveolar macrophages in mouse lung and that bleomycin-induced lung damage is more severe in *Angptl2* KO than in wild-type mice. Based also on results seen following BMT, we propose that ANGPTL2 production by lung epithelial cells is important for tissue repair after bleomycin-induced damage.

We previously reported that ANGPTL2 is a proinflammatory mediator (1, 2, 20, 41). Specifically, unregulated ANGPTL2 expression led to chronic inflammation, resulting in obesity-related insulin resistance (41), type II diabetes (41), atherosclerosis (20), and carcinogenesis (1, 2). Thus, we hypothesized that ANGPTL2 expression in mice might worsen pathological conditions associated with interstitial pneumonia induced by bleomycin. Therefore, the finding reported here that lung damage is more severe and lethal (data not shown) in *Angptl2* KO relative to wild-type mice is unanticipated. One explanation for this observation is that, in general, a moderate inflammatory response is required to repair damaged tissues and maintain tissue homeostasis following injury (47). We conclude that ANGPTL2 secreted by lung epithelial cells may serve that protective function in lung.

Culture of 3T3-L1 cells with mouse rANGPTL2 repressed induction of *TSP1*, *COL1A1*, and *COL1A2*, suggesting that ANGPTL2 protein inhibits a fibrotic response. Integrins reportedly regulate fibrosis by activating TGF-β (18). Specifically, activation of integrins αvβ6, αvβ8, and α3β1 promotes fibrosis (24, 25, 27, 31). TSP1 is downregulated by CCAAT-enhancer-binding protein (CEBP) δ (7), and integrin signaling activates CEBPs (40). We showed previously that ANGPTL2 binds to integrin α5β1 (41), which is expressed on fibroblasts (28) and lung epithelial cells (19, 39). Therefore, we hypothesize that ANGPTL2 may signal through integrin α5β1 or an as yet unidentified integrin expressed on fibroblasts to inhibit *TSP1* mRNA induction or block TGF-β activation. These possibilities should be tested in future studies.

TSP1 is a regulatory factor that activates TGF-β (32), and conversely, inhibition of TSP1 synthesis suppresses TGF-β activity (8). On the other hand, *TSP1* KO does not protect mice from lung fibrosis (14). Thus, other regulatory factors known to activate TGF-β (9) may be regulated by ANGPTL2. Further analysis is required to confirm which signal pathways mediate the protective effects of ANGPTL2.

In some chronic diseases, ANGPTL2 appears to promote fibrosis by inducing TGF-related genes (30, 33). Although

Downloaded from journals.physiology.org/journal/ajplung (065.021.193.086) on March 8, 2022.

these activities seem contradictory, the potency of a fibrotic response may depend on the microenvironment and whether there is persistent or transient inflammation. Persistent inflammation causes epigenetic changes reportedly related to fibrosis (10, 45). The mouse bleomycin-induced fibrosis model examined here is a short-term experiment; thus, our results may reflect transient effects of ANGPTL2, although this possibility requires further analysis.

In summary, we show that ANGPTL2 may function in preventing lung fibrosis. Our data also suggest that ANGPTL2 upregulation in lung could be useful in protecting against fibrosis, although a caveat is that prolonged ANGPTL2 expression in lung could be a cancer risk (1, 2). Thus, it may be necessary to develop a way to administer appropriate levels of ANGPTL2 before this approach can be applied as therapy to treat lung fibrosis.

ACKNOWLEDGMENTS

We thank K. Tabu, M. Nakata, and N. Shirai for technical assistance.

GRANTS

This work was supported by the Scientific Research Fund of the Ministry of Education, Culture, Sports, Science, and Technology of Japan (Grants Nos. 25461192, 15K09180, and 15H01159), by the Core Research for Evolutional Science and Technology (CREST) program of the Japan Science and Technology Agency (Grant No. 13417915), and by the CREST program of the Japan Agency for Medical Research and Development (Grant No. 15gm0610007h0003).

DISCLOSURES

No conflicts of interest, financial or otherwise are declared by the authors.

AUTHOR CONTRIBUTIONS

I. Motokawa, M.E., T.I., H.I., and Y.O. conception and design of research; I. Motokawa, M.E., K.T., H.H., K.M., and M.S.M. performed experiments; I. Motokawa, M.E., K.T., H.H., T.K., M.S.M., I. Manabe, T. Samukawa, and M.W. analyzed data; I. Motokawa, M.E., T.K., J.M., T. Sugizaki, T.I., K.A., I. Manabe, H.I., and Y.O. interpreted results of experiments; I. Motokawa, M.E., and K.T. prepared figures; I. Motokawa and M.E. drafted manuscript; I. Motokawa, M.E., K.T., H.I., and Y.O. edited and revised manuscript; I. Motokawa, M.E., K.T., H.H., K.M., T.K., J.M., T. Sugizaki, T.I., K.A., M.S.M., I. Manabe, T. Samukawa, M.W., H.I., and Y.O. approved final version of manuscript.

REFERENCES

1. **Aoi J, Endo M, Kadomatsu T, Miyata K, Nakano M, Horiguchi H, Ogata A, Odagiri H, Yano M, Araki K, Jinnin M, Ito T, Hirakawa S, Ihn H, Oike Y.** Angiopoietin-like protein 2 is an important facilitator of inflammatory carcinogenesis and metastasis. *Cancer Res* 71: 7502–7512, 2011.
2. **Aoi J, Endo M, Kadomatsu T, Miyata K, Ogata A, Horiguchi H, Odagiri H, Masuda T, Fukushima S, Jinnin M, Hirakawa S, Sawa T, Akaike T, Ihn H, Oike Y.** Angiopoietin-like protein 2 accelerates carcinogenesis by activating chronic inflammation and oxidative stress. *Mol Cancer Res* 12: 239–249, 2014.
3. **Audic S, Claverie J.** The significance of digital gene expression profiles. *Genome Res* 7: 986–995, 1997.
4. **Benjamini Y, Hochberg Y.** Controlling the false discovery rate: a practical and powerful approach to multiple testing. *J Roy Stat Soc B* 57: 289–300, 1995.
5. **Boorsma C, Draijer C, Melgert B.** Macrophage heterogeneity in respiratory diseases. *Mediators Inflamm* 27, 2013.
6. **Chambers R, Mercer P.** Mechanisms of alveolar epithelial injury, repair, and fibrosis. *Ann Am Thorac Soc* 12: S16–S20, 2015.
7. **Chu Y, Ko C, Wang W, Wang S, Gean P, Kuo Y, Wang J.** Astrocytic CCAAT/enhancer binding protein delta regulates neuronal viability and spatial learning ability via miR-135a. *Mol Neurobiol* 53: 4173–4188, 2016.
8. **Daniel C, Takabatake Y, Mizui M, Isaka Y, Kawashi H, Rupprecht H, Imai E, Hugo C.** Antisense oligonucleotides against thrombospondin-1 inhibit activation of tgf-beta in fibrotic renal disease in the rat in vivo. *Am J Pathol* 163: 1185–1192, 2003.
9. **Di GG.** TSP-1 in lung fibrosis. *J Cell Commun Signal* 4: 185–186, 2010.
10. **Dowson C, O' Reilly S.** DNA methylation in fibrosis. *Eur J Cell Biol* 003, 2016.
11. **Endo M, Mori M, Akira S, Gotoh T.** C/EBP homologous protein (CHOP) is crucial for the induction of caspase-11 and the pathogenesis of lipopolysaccharide-induced inflammation. *J Immunol* 176: 6245–6253, 2006.
12. **Endo M, Nakano M, Kadomatsu T, Fukuhara S, Kuroda H, Mikami S, Hato T, Aoi J, Horiguchi H, Miyata K, Odagiri H, Masuda T, Harada M, Horio H, Hishima T, Nomori H, Ito T, Yamamoto Y, Minami T, Okada S, Takahashi T, Mochizuki N, Iwase H, Oike Y.** Tumor cell-derived angiopoietin-like protein ANGPTL2 is a critical driver of metastasis. *Cancer Res* 72: 1784–1794, 2012.
13. **Endo M, Oyadomari S, Terasaki Y, Takeya M, Suga M, Mori M, Gotoh T.** Induction of arginase I and II in bleomycin-induced fibrosis of mouse lung. *Am J Physiol Lung Cell Mol Physiol* 285: L313–L321, 2003.
14. **Ezzie M, Piper M, Montague C, Newland C, Opalek J, Baran C, Ali N, Brigstock D, Lawler J, Marsh C.** Thrombospondin-1-deficient mice are not protected from bleomycin-induced pulmonary fibrosis. *Am J Respir Cell Mol Biol* 44: 556–561, 2011.
15. **Fernandez I, Eickelberg O.** New cellular and molecular mechanisms of lung injury and fibrosis in idiopathic pulmonary fibrosis. *Lancet* 380: 680–688, 2012.
16. **Fernandez Perez E, Daniels C, Schroeder D, St Sauver J, Hartman T, Bartholmai B, Yi E, Ryu J.** Incidence, prevalence, and clinical course of idiopathic pulmonary fibrosis: a population-based study. *Chest* 137: 129–137, 2010.
17. **Gomperts B, Strieter R.** Fibrocytes in lung disease. *J Leukoc Biol* 82: 449–456, 2007.
18. **Henderson N, Sheppard D.** Integrin-mediated regulation of TGFβ in fibrosis. *Biochim Biophys Acta* 6, 2013.
19. **Herard A, Pierrot D, Hinnrasky J, Kaplan H, Sheppard D, Puchelle E, Zahm J.** Fibronectin and its α5β1-integrin receptor are involved in the wound-repair process of airway epithelium. *Am J Physiol Lung Cell Mol Physiol* 271: L726–L733, 1996.
20. **Horio E, Kadomatsu T, Miyata K, Arai Y, Hosokawa K, Doi Y, Ninomiya T, Horiguchi H, Endo M, Tabata M, Tazume H, Tian Z, Takahashi O, Terada K, Takeya M, Hao H, Hirose N, Minami T, Suda T, Kiyohara Y, Ogawa H, Kaikita K, Oike Y.** Role of endothelial cell-derived angptl2 in vascular inflammation leading to endothelial dysfunction and atherosclerosis progression. *Arterioscler Thromb Vasc Biol* 34: 790–800, 2014.
21. **Jones M, Fletcher S, Richeldi L.** Idiopathic pulmonary fibrosis: recent trials and current drug therapy. *Respiration* 86: 353–363, 2013.
22. **Kadomatsu T, Endo M, Miyata K, Oike Y.** Diverse roles of ANGPTL2 in physiology and pathophysiology. *Trends Endocrinol Metab* 25: 245–254, 2014.
23. **Kim H, Perlman D, Tomic R.** Natural history of idiopathic pulmonary fibrosis. *Respir Med* 002, 2015.
24. **Kim K, Wei Y, Szekeres C, Kugler M, Wolters P, Hill M, Frank J, Brumwell A, Wheeler S, Kreidberg J, Chapman H.** Epithelial cell α3β1 integrin links beta-catenin and Smad signaling to promote myofibroblast formation and pulmonary fibrosis. *J Clin Invest* 119: 213–224, 2009.
25. **Kitamura H, Cambier S, Somanath S, Barker T, Minagawa S, Markovics J, Goodsell A, Publicover J, Reichardt L, Jablons Dl Wolters P, Hill A, Marks J, Lou J, Pittet J, Gauldie J, Baron J, Nishimura S.** Mouse and human lung fibroblasts regulate dendritic cell trafficking, airway inflammation, and fibrosis through integrin αvβ8-mediated activation of TGF-β. *J Clin Invest* 121: 2863–2875, 2011.
26. **Konigshoff M, Kramer M, Balsara N, Wilhelm J, Amarie O, Jahn A, Rose F, Fink L, Seeger W, Schaefer L, Gunther A, Eickelberg O.** WNT1-inducible signaling protein-1 mediates pulmonary fibrosis in mice and is upregulated in humans with idiopathic pulmonary fibrosis. *J Clin Invest* 119: 772–787, 2009.
27. **Liu S, Kapoor M, Denton C, Abraham D, Leask A.** Loss of β1 integrin in mouse fibroblasts results in resistance to skin scleroderma in a mouse model. *Arthritis Rheum* 60: 2817–2821, 2009.
28. **Lobert V, Brech A, Pedersen N, Wesche J, Oppelt A, Malerod L, Stenmark H.** Ubiquitination of α5β1 integrin controls fibroblast migra-

Downloaded from journals.physiology.org/journal/ajplung (065.021.193.086) on March 8, 2022.

tion through lysosomal degradation of fibronectin-integrin complexes. *Dev Cell* 19: 148–159, 2010.
29. **Masuda T, Endo M, Yamamoto Y, Odagiri H, Kadomatsu T, Nakamura T, Tanoue H, Ito H, Yugami M, Miyata K, Morinaga J, Horiguchi H, Motokawa I, Terada K, Morioka M, Manabe I, Iwase H, Mizuta H, Oike Y.** ANGPTL2 increases bone metastasis of breast cancer cells through enhancing CXCR4 signaling. *Sci Rep* 5: 2015.
30. **Morinaga J, Kadomatsu T, Miyata K, Endo M, Terada K, Tian Z, Sugizaki T, Tanigawa H, Zhao J, Zhu S, Sato M, Araki K, Iyama K, Tomita K, Mukoyama M, Tomita K, Kitamura K, Oike Y.** Angiopoietin-like protein 2 increases renal fibrosis by accelerating transforming growth factor-β signaling in chronic kidney disease. *Kidney Int* 89: 327–341, 2016.
31. **Munger J, Huang X, Kawakatsu H, Griffiths M, Dalton S, Wu J, Pittet J, Kaminski N, Garat C, Matthay M, Rifkin D, Sheppard D.** The integrin αvβ6 binds and activates latent TGFβ1: a mechanism for regulating pulmonary inflammation and fibrosis. *Cell* 96: 319–328, 1999.
32. **Murphy-Ullrich J, Poczatek M.** Activation of latent TGF-β by thrombospondin-1: mechanisms and physiology. *Cytokine Growth Factor Rev* 11: 59–69, 2000.
33. **Nakamura T, Okada T, Endo M, Kadomatsu T, Taniwaki T, Sei A, Odagiri H, Masuda T, Fujimoto T, Nakamura T, Oike Y, Mizuta H.** Angiopoietin-like protein 2 induced by mechanical stress accelerates degeneration and hypertrophy of the ligamentum flavum in lumbar spinal canal stenosis. *PLoS One* 9: 2014.
34. **Odagiri H, Kadomatsu T, Endo M, Masuda T, Morioka M, Fukuhara S, Miyamoto T, Kobayashi E, Miyata K, Aoi J, Horiguchi H, Nishimura N, Terada K, Yakushiji T, Manabe I, Mochizuki N, Mizuta H, Oike Y.** The secreted protein ANGPTL2 promotes metastasis of osteosarcoma cells through integrin α5β1, p38 MAPK, and matrix metalloproteinases. *Sci Signal* 7: 2004612, 2014.
35. **Ogata A, Endo M, Aoi J, Takahashi O, Kadomatsu T, Miyata K, Tian Z, Jinnin M, Fukushima S, Ihn H, Oike Y.** The role of angiopoietin-like protein 2 in pathogenesis of dermatomyositis. *Biochem Biophys Res Commun* 418: 494–499, 2012.
36. **Okada T, Tsukano H, Endo M, Tabata M, Miyata K, Kadomatsu T, Miyashita K, Semba K, Nakamura E, Tsukano M, Mizuta H, Oike Y.** Synoviocyte-derived angiopoietin-like protein 2 contributes to synovial chronic inflammation in rheumatoid arthritis. *Am J Pathol* 176: 2309–2319, 2010.
37. **Quinlan A, Hall I.** BEDTools: a flexible suite of utilities for comparing genomic features. *Bioinformatics* 26: 841–842, 2010.
38. **Schneider D, Wu M, Le T, Cho S, Brenner M, Blackburn M, Agarwal S.** Cadherin-11 contributes to pulmonary fibrosis: potential role in TGF-β production and epithelial to mesenchymal transition. *FASEB J* 26: 503–512, 2012.
39. **Sheppard D.** Functions of pulmonary epithelial integrins: from development to disease. *Physiol Rev* 83: 673–686, 2003.
40. **Stupack D, Cheresh D.** Get a ligand, get a life: integrins, signaling and cell survival. *J Cell Sci* 115: 3729–3738, 2002.
41. **Tabata M, Kadomatsu T, Fukuhara S, Miyata K, Ito Y, Endo M, Urano T, Zhu H, Tsukano H, Tazume H, Kaikita K, Miyashita K, Iwawaki T, Shimabukuro M, Sakaguchi K, Ito T, Nakagata N, Yamada T, Katagiri H, Kasuga M, Ando Y, Ogawa H, Mochizuki N, Itoh H, Sud aT, Oike Y.** Angiopoietin-like protein 2 promotes chronic adipose tissue inflammation and obesity-related systemic insulin resistance. *Cell Metab* 10: 178–188, 2009.
42. **Tazume H, Miyata K, Tian Z, Endo M, Horiguchi H, Takahashi O, Horio E, Tsukano H, Kadomatsu T, Nakashima Y, Kunitomo R, Kaneko Y, Moriyama S, Sakaguchi H, Okamoto K, Hara M, Yoshinaga T, Yoshimura K, Aoki H, Araki K, Hao H, Kawasuji M, Oike Y.** Macrophage-derived angiopoietin-like protein 2 accelerates development of abdominal aortic aneurysm. *Arterioscler Thromb Vasc Biol* 32: 1400–1409, 2012.
43. **Terzyan SS, Peracaula R, de Llorens R, Tsushima Y, Yamada H, Seno M, Gomis-Ruth FX, Coll M.** The three-dimensional structure of human RNase 4, unliganded and complexed with d(Up), reveals the basis for its uridine selectivity. *J Mol Biol* 285: 205–214, 1999.
44. **Trapnell C, Pachter L, Salzberg S.** TopHat: discovering splice junctions with RNA-Seq. *Bioinformatics* 25: 1105–1111, 2009.
45. **Tzouvelekis A, Kaminski N.** Epigenetics in idiopathic pulmonary fibrosis. *Biochem Cell Biol* 93: 159–170, 2015.
46. **Uhal B, Kim J, Li X, Molina-Molina M.** Angiotensin-TGF-β1 crosstalk in human idiopathic pulmonary fibrosis: autocrine mechanisms in myofibroblasts and macrophages. *Curr Pharm Des* 13: 1247–1256, 2007.
47. **Wynn T.** Integrating mechanisms of pulmonary fibrosis. *J Exp Med* 208: 1339–1350, 2011.
48. **Yugami M, Odagiri H, Endo M, Tsutsuki H, Fujii S, Kadomatsu T, Masuda T, Miyata K, Terada K, Tanoue H, Ito H, Morinaga J, Horiguchi H, Sugizaki T, Akaike T, Gotoh T, Takai T, Sawa T, Mizuta H, Oike Y.** Mice deficient in Angptl2 show increased susceptibility to bacterial infection due to attenuated macrophage activity. *J Biol Chem* 291: 18843–18852, 2016.
49. **Zemans R, Colgan S, Downey G.** Transepithelial migration of neutrophils: mechanisms and implications for acute lung injury. *Am J Respir Cell Mol Biol* 40: 519–535, 2009.

Downloaded from journals.physiology.org/journal/ajplung (065.021.193.086) on March 8, 2022.